ISSN: 1813-4890

Wideband High Gain Filtering Vivaldi Antenna Design Based on spoof surface plasmon polaritons Structure

Weiping Xiao

Tianjin University of Technology and Education, Hexi, Tianjin, China

xiaoxiaode2023@163.com

Abstract

In this paper, a wideband high-gain filtering Vivaldi antenna is proposed. In this design, the spoof surface plasmon polaritons （SSPPs） structure with inherent dispersion is etched on the slot line to realize the filtering, and the SSPP structure at the front end of the Vivaldi antenna is used as an equivalent lens to improve the gain. A set of V-shaped slots etched on the outer edge of the antenna to reduce diffraction current and further improves the gain and front-to-back ratio . The measurement results show that high gain performance over the wide frequency range from 14.5GHz to 25.6 GHz, with a maximum gain of 11.4dBi.

Keywords

Vivaldi antenna, spoof surface plasmon polaritons (SSPPs), high gain.

1. Introduction

In modern communication systems, wideband high-gain Vivaldi antennas have been widely used in radar [1]and satellite communication [2-4]. Its excellent performance and flexibility make Vivaldi antennas ideal for high-speed data transmission and complex communication needs. Due to its simple structure, Vivaldi antennas are able to achieve high gain in different frequency bands. [5-6] utilizes metasurface consisting of cells is loaded in front of the antenna to unify the phase distribution. After careful design, changing the phase and amplitude of the wave to control the electromagnetic (EM) wave, the radiation performance is significantly improved in the wide band, [7] adding dielectric lenses at the front end of the antenna, in addition, adding parasitic units [8] is also an effective way to improve the radiation performance

Artificial Surface Plasmon Polaritons (SSPPs) [9] are a type of surface wave that exists at the interface between a dielectric material and a metal surface it has been widely applied in various filtering devices, splitters, and antennas. Sspps achieves different dispersion characteristics by adjusting the depth of grooves[10-11] to match applicable frequencies. [12] has proposed a Vivaldi antenna with filtering capabilities; however, there is still significant room for improvement in its gain.

In this paper, a wideband high gain filtering Vivaldi antenna is proposed. To maximize the gain performance, an equivalent lens structure based on the Surface Plasmon Polaritons (SPP) is employed in front of the Vivaldi antenna. This significantly enhances the antenna performance within a wide frequency range of 14.5 GHz to 25.6GHz, demonstrating excellent radiation characteristics with a peak gain of 11.4dBi. In comparison to Reference [12], the average gain within the bandwidth is increased by 1.3 dBi, with a peak gain enhancement of 1.5 dBi.

ISSN: 1813-4890

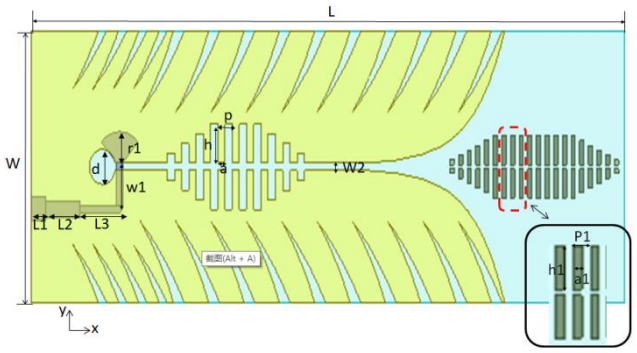

Fig. 1. Configuration of the proposed antenna. Dimensions: w=41, l=14, l1=1.2, l2=2.4,l3=2.9,w1=2.48,w2=0.4,r1=1.8,d=1.8,p=1,a=0.5,h=2.0,p1=0.6,a1=0.3,h1= 1.5(unit: mm).

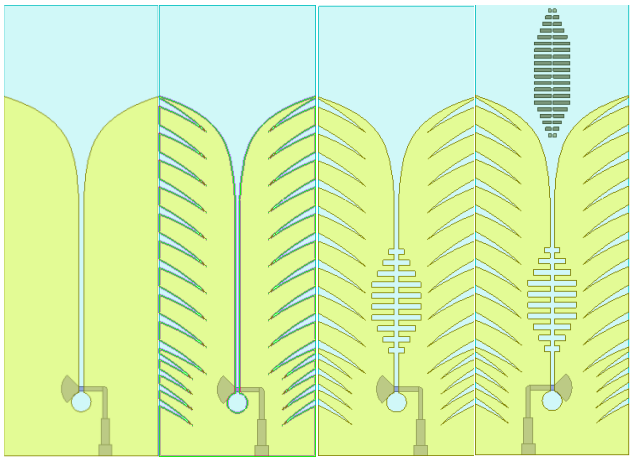

(a) (b) (c) (d)

Fig. 2. The evolution process of the proposed antenna. (a) ANT Ⅰ. (b) ANT Ⅱ. (c) ANT Ⅲ. (d) ANT Ⅳ.

2. Antenna design

The proposed antenna structure as shown in Fig.1, in which the key components are enlarged for clarity.Fig.2 presents the evolutionary process of the proposed antenna. ANT Ⅰ is a traditional Vivaldi antenna implemented on Rogers 4003C substrate with a relative permittivity of 2.2 and thickness of 0.5 mm. The antenna is fed from the bottom by a feed network composed of a gradient L-shaped microstrip. ANT Ⅱ is a V-shaped slot etched into the outer edge of ANT Ⅰ, ANT Ⅲ is the etching of SSPP structure with inherent dispersion on the slot line of ANT Ⅱ. Finally, The equivalent lens composed of SSPPs is loaded on the front end of ANT Ⅲ to form ANT Ⅳ.

In order to reduce the unwanted derived current at both ends of the antenna, a set of V-shaped slots was etched at the external edges of ANT Ⅰ. the radiation patterns for ANT Ⅰ and ANT Ⅱ at 23 GHz as shown in Fig 3. The main lobe gain increased by 2 dBi, and the accompanying side lobe levels improved significantly, greatly optimizing the antenna's performance. ANT Ⅲ has a series of rectangular patches arranged in a regular pattern are etched on the slot lines to achieve filtering. This sspps structure has inherent dispersion properties.To achieve broadband matching of wave vectors and impedances between the slot lines and the SSPP waveguide, a gradient transition was employed.

The SSPP structures with different lengths(h) of rectangular patches have varying cutoff frequencies. When the frequency is lower than the plasma cutoff frequency, SSPP waves can

ISSN: 1813-4890

propagate smoothly; however, when the frequency is higher than the plasma cutoff frequency, the propagation of SSPP waves is blocked.Fig.4 shows the electric field distributions of ANT Ⅲ at 23 GHz and 27 GHz, where SSPP wave propagation is terminated at 27 GHz. Its unique dispersion characteristics enable convenient control of the cutoff frequency By adjusting the length of the rectangular patches, achieving filtering effects .the Fig.5 can be observed that the gain of ANT Ⅲ rapidly drops below -4 dBi at 25.6 GHz.

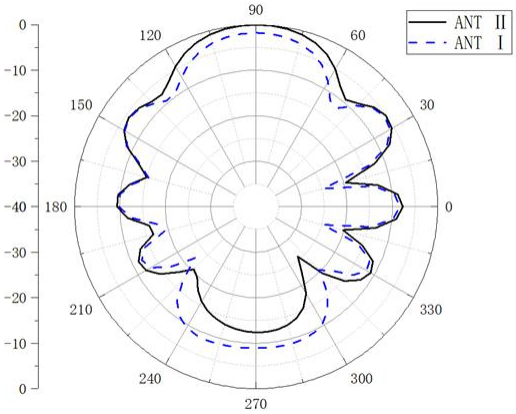

Fig.3. The radiation pattern (E-plane) comparison of the antenna at 23GHz.

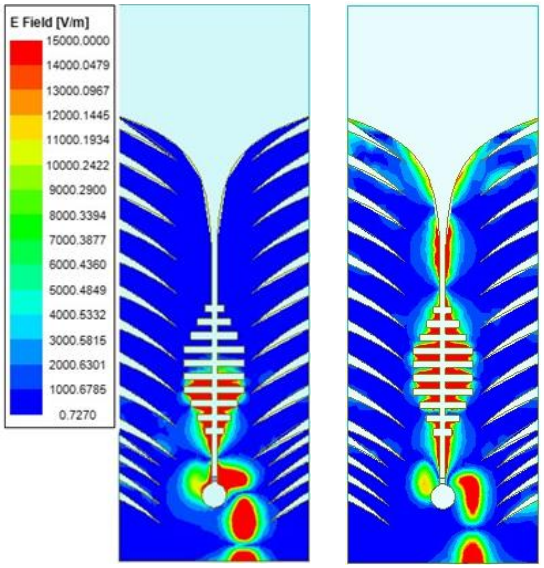

(b)

Fig.4.The simulated E-fields of ANT Ⅲ (a) 23 GHz, (b) 27GHz.

Additionally, a decrease in gain performance is noted at 17.5 GHz, Furthermore, the gain performance can be observed to decline at 17.5GHz, which is to be expected. a low cutoff frequency limited by the antenna aperture width, causing degradation of the reflection coefficient within the frequency range of 12.5-14.5 GHz (Fig. 6).Figure 6 illustrates the impact of the SSPP structure's ength (h) on the antenna Filtering

ISSN: 1813-4890

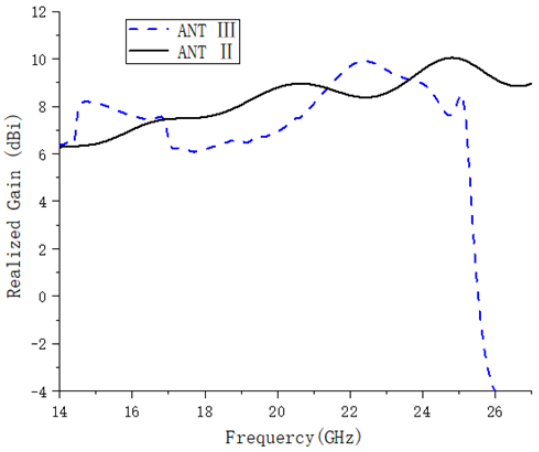

Fig.5. The simulated gain performances of ANT Ⅱ and ANT Ⅲ

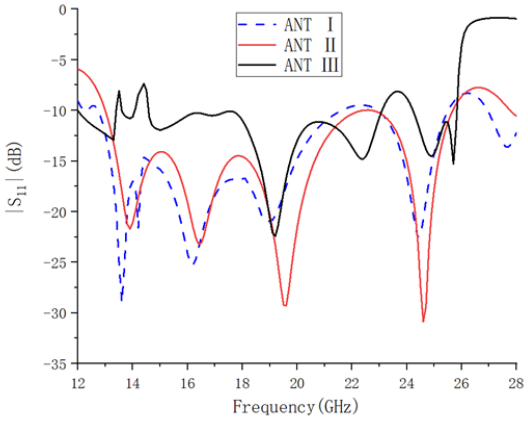

Fig.6. The simulated reflection coefficients(S11)

performance. Due to the inherent dispersion characteristics of the SSPP structure, as 'h' increases, its cutoff frequency gradually decreases. In the figure, the antenna gain rapidly drops below -4 dBi at 12 GHz, 21 GHz, and 21 GHz respectively when 'h' increased. Therefore, the antenna filtering frequency can be controlled by changing the plasma length 'h.In order to achieve the ideal broadband high gain performance, a plasmon lens is designed by using strong field confinement properties of artificial surface plasmon. Etched regularly

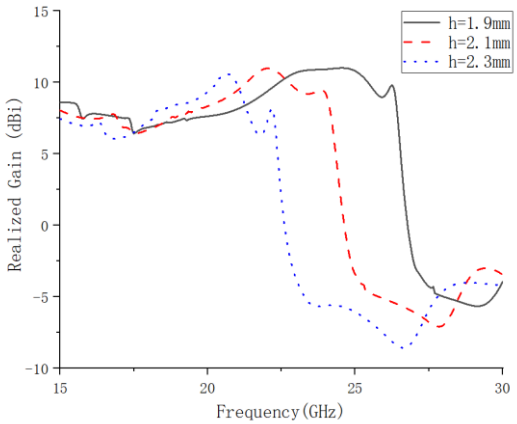

Fig.7 .The Simulation of gain at different lengths h

ISSN: 1813-4890

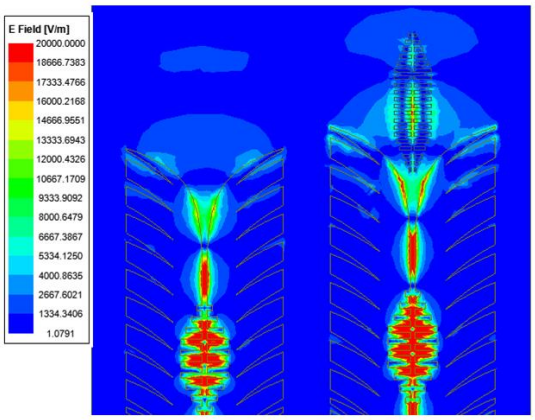

Fig.8.The simulated E-fields of ANT Ⅲ and ANT Ⅳ

arranged rectangular pieces with gradient transitions in front and back.. Fig. 7 shows the electric field of the antenna with and without the plasmon lens loaded at 23ghz.It can be clearly seen from the figure that after loading the lens, the Antenna radiation field is more concentrated in the front end of the antenna. It can be observed from Figure 9 that after loading the lens, the average antenna gain increases by 1.36dbi and the maximum gain increases by 1.58dbi in the entire bandwidth, and the antenna reflection coefficient is also slightly improved.

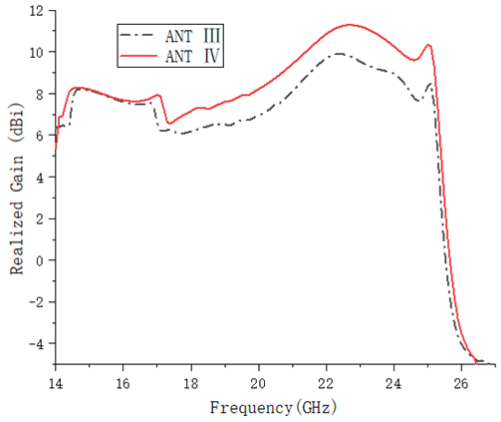

Fig.9. The Simulation of gain at ANT Ⅲ and ANT Ⅳ

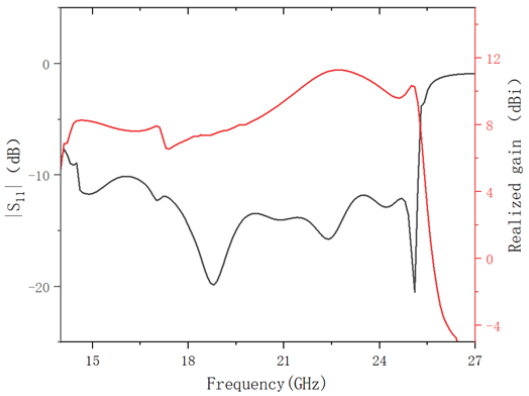

Fig.10. The Simulation of gain and reflection coefficients

3. Conclution

A wideband high gain filtering Vivaldi antenna is designed, a set of V-shaped slots was etched at the outer edges of the antenna to reduce surface diffraction currents. To achieve filtering effects, the SSPP structure with inherent dispersion characteristic etched in the slot-line, and a

ISSN: 1813-4890

gradient transition was applied for wideband match. To further enhance the broadband gain, a novel plasma element lens was introduced. The simulated S-parameters and gain of the antenna are shown in Figure 10. The results indicate an impedance bandwidth with |S11| < -10 dB from 14.5. GHz to 26.65 GHz. Within this bandwidth, the gain varies from 7.2 to 11.39dBi. Fig.11 displays the normalized simulated radiation patterns of the antenna at 16 GHz 29 GHz and 21 GHz. The antenna exhibits excellent radiation characteristics within its bandwidth, making it a broadband antenna that is easy to fabricate and assemble. This Vivaldi antenna demonstrates promising applications in the design of antennas with wide bandwidth, high gain, and excellent radiation performance.

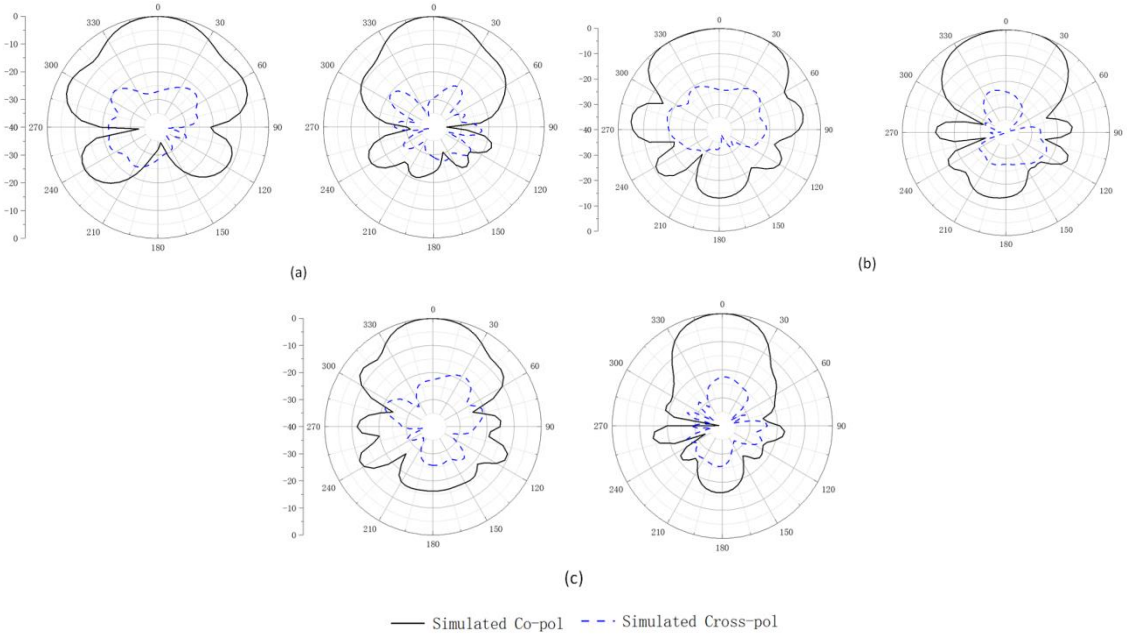

Fig.11. The normalized simulated radiation patterns of the antenna. (a) 16 GHz, and (b) 19 GHz (c)22GHz .

References

[1] J. Yu, W. Jiang and S. Gong, "Low-RCS Beam-Steering Antenna Based on Reconfigurable Phase Gradient Metasurface," in IEEE Antennas and Wireless Propagation Letters, vol. 18, no. 10, pp. 2016-2020, Oct. 2019, doi: 10.1109/LAWP.2019.2936300.

[2] T. Zhang, Y. Chen, Z. Liu and S. Yang, "A Low-Scattering Vivaldi Antenna Array With Slits on Nonradiating Edges," in IEEE Transactions on Antennas and Propagation, vol. 71, no. 2, pp. 1999-2004, Feb. 2023, doi: 10.1109/TAP.2022.3232690.

[3] K. Zhang, R. Tan, Z. H. Jiang, Y. Huang, L. Tang and W. Hong, "A Compact, Ultrawideband Dual-Polarized Vivaldi Antenna With Radar Cross Section Reduction," in IEEE Antennas and Wireless Propagation Letters, vol. 21, no. 7, pp. 1323-1327, July 2022, doi: 10.1109/LAWP.2022.3166821.

[4] H. -T. Chou and Y. -J. Lin, "An Optimum Design of Paired Balanced Antipodal Vivaldi Antennas With Mirror-Imaged Symmetric Architectures for Ultra-Broadband Characteristics From Microwave to Millimeter-Wave Frequency Ranges," in IEEE Access, vol. 10, pp. 99516-99524, 2022, doi: 10.1109/ACCESS.2022.3206914.

[5] M. T. Islam, M. T. Islam, M. Samsuzzaman, H. Arshad and H. Rmili, "Metamaterial Loaded Nine High Gain Vivaldi Antennas Array for Microwave Breast Imaging Application," in IEEE Access, vol. 8, pp. 227678-227689, 2020, doi: 10.1109/ACCESS.2020.3045458.

[6] M. Singh and M. S. Parihar, "Gain Improvement of Vivaldi MIMO Antenna With Pattern Diversity Using Bi-Axial Anisotropic Metasurface for Millimeter-Wave Band Application," in IEEE Antennas and Wireless Propagation Letters, vol. 22, no. 3, pp. 621-625, March 2023, doi: 10.1109/LAWP.2022.3220710.

[7] J. Xu and Z. Zheng, "High-Gain and Wideband Planar Endfire Antenna Implemented via Spoof Surface Plasmon Polaritons and Dielectric Lens for X-Band Applications," in IEEE Antennas and Wireless Propagation Letters, vol. 22, no. 2, pp. 382-386,Feb.2023, doi: 10.1109/LAWP.2022.3213553

[8] R. Elmahraoui, R. Rais and T. Mourabit, "A New Endfire Phased Array based on Vivaldi Antenna for 5G Applications," 2021 IEEE 19th International Symposium on Antenna Technology and Applied Electromagnetics (ANTEM), Winnipeg, MB, Canada, 2021,pp.1-2,do

[9] D. Cao, Y. Li and J. Wang, "A Millimeter-Wave Spoof Surface Plasmon Polaritons-Fed Microstrip Patch Antenna Array," in IEEE Transactions on Antennas and Propagation, vol. 68, no. 9, pp. 6811-6815, Sept. 2020, doi: 10.1109/TAP.2020.2972696.

[10] X. Du, J. Ren, H. Li, C. Zhang, Y. Liu and Y. Yin, "Design of a Leaky-Wave Antenna Featuring Beam Scanning From Backfire Utilizing Odd-Mode Spoof Surface Plasmon Polaritons," in IEEE Transactions on Antennas and Propagation, vol. 69, no. 10, pp. 6971-6976, Oct. 2021, doi: 10.1109/TAP.2021.3076166.

[11] Y. Wu et al., "Design of Quasi-Endfire Spoof Surface Plasmon Polariton Leaky-Wave Textile Wearable Antennas," in IEEE Access, vol. 10, pp. 115338-115350, 2022, doi: 10.1109/ACCESS.2022.3218217.

[12] H. Qi and H. Liu, "Wideband High-Gain Filtering Vivaldi Antenna Design Based on MS and Herringbone SSPP Structure," in IEEE Antennas and Wireless Propagation Letters, vol. 22, no. 8, pp. 1798-1802, Aug. 2023, doi: 10.1109/LAWP.2023.3264702.